

Marek SZCZEPAŃSKI
Politechnika Śląska

FAST DIGITAL PATHS APPROACH SPATIO-TEMPORAL FILTER

Summary. A new efficient spatio-temporal filtering technique for off-line video enhancement was presented in this paper. The new approach is based on digital paths concepts [16, 17] in three dimensional space. The digital paths can explore image structures in spatial as well as temporal coordinates from subsequent frames.

Presented technique copes with different video artifacts such as Gaussian, impulsive and grain noise and still preserves and even enhances edges.

CZASOWO-PRZESTRZENNY FILTR FDPA

Streszczenie. Artykuł przedstawia nową, efektywną metodę filtracji barwnych sekwencji wideo. Zaproponowany algorytm wykorzystuje ideę ścieżek cyfrowych w trójwymiarowej przestrzeni. Ścieżki cyfrowe eksplorują struktury obrazu zarówno w czasie, jak i w przestrzeni, co zapewnia doskonałe zachowanie detali obrazu oraz zapobiega powstawaniu artefaktów związanych z uśrednianiem ruchomych obiektów pomiędzy kolejnymi klatkami. Zaprezentowana technika skutecznie usuwa szum gaussowski, impulsowy oraz artefakty kompresji, zachowując, a nawet poprawiając krawędzie w obrazie.

1. Introduction

From several years we can observe increasing interest in video processing. Video noise reduction without structure degradation is perhaps the most challenging video enhancements task.

There are several sources of video noise such us:

- sensor noise - especially visible in cheap cameras and in low light vision tasks,
- digital compression artifacts - blocking, ringing
- transmission artifacts
- film artifact - dust, scratches, fingerprints and grain noise - those artifacts are really important in old movies restoration.

Several techniques have been proposed over the years. Among them are standard noise reduction techniques, the so-called spatial filters, applied to subsequent frames of the video stream.

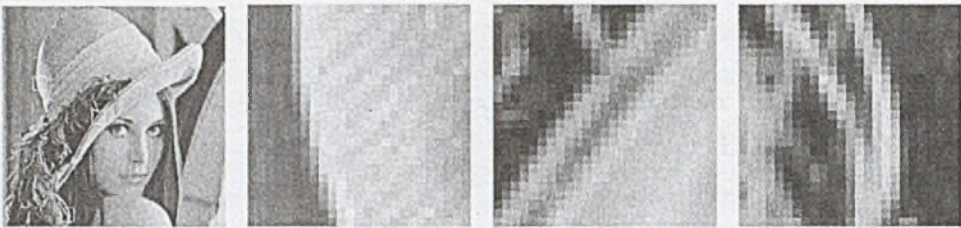


Fig. 1. Paths in the test image *LENA*

However, standard image processing techniques cannot utilize all available information i.e. similarities in neighboring frames.

Modern video denoising algorithms can be divided into three basic groups:

- spatial - standard noise reduction techniques, all frames are processed separately
- temporal - only temporal information is used,
- spatio-temporal - combination of spatial and temporal denoising.

In this paper we propose a different approach. We propose to exploit possible connections between successive image pixels using the concept of digital paths in spatial domain which can be extended to temporal domain and understood as trajectories or object displacements in subsequent frames.

After analyzing some natural images one could find that pixels form some kind of "paths", especially in textures and on the fine image details. Examples of such "paths" in famous test image *LENA* are presented in Fig. 1.

According to the proposed here methodology, image pixels are grouped together forming paths that reveal the underlying structural dynamics of the image.

The path displacements evaluated over all possible digital paths, are used to derive fuzzy membership functions that quantify similarity between vectorial inputs. The proposed filtering structure is then using the function outputs to appropriately weight input contributions in order to determine the filtered result.

The proposed filtering technique can successfully eliminate Gaussian and impulsive noise as well as digital compression artifacts. However, thanks to the introduction of the digital paths in its supporting element, the new filters not only preserve the edges and the other fine details in the image, but it is possible to enhance them acting as an image sharpening operators.

Some temporal filters can introduce strong ghosting artifacts from moving objects [2], however tracking capabilities of digital paths reduce to minimum.

The paper is organized as follows. In Section 2.2. the general concept of the digital paths applied to the spatial filters is introduced. Section 3.3. introduces concept of our spatio-temporal filter, while Section 4 presents simulation results. Finally, Section 5 summarizes our paper.

2. Spatial Fast Digital Paths Approach Filter (FDPA)

2.1. General filter framework

In this work general fuzzy filtering structure proposed in [7, 8, 10] will be used. The general form of the fuzzy adaptive filters proposed in this work is defined as weighted average of input vectors inside the processing window W .

$$\hat{F}_0 = \sum_{i=0}^{k-1} w_i F_i = \frac{\sum_{i=0}^{k-1} \mu_i F_i}{\sum_{i=0}^{k-1} \mu_i}, \quad (1)$$

where F_i and \hat{F}_0 denotes filter inputs and output respectively.

The relationship between the pixel under consideration (window center) and each pixel in the window should be reflected in the decision how to define the filter weights. In our case weights will be calculated using similarity functions calculated over digital paths included in the processing window W .

In order to simplify implementation of algorithms and make them faster the path length will be fixed to the certain value n . In such case algorithms will consider only paths of length n .

Using the connection cost function concept it is possible to define different classes of similarity functions. Choosing a specific form of similarity function yields different filter classes, with different properties which can be applied for various low level vision tasks.

2.2. Connection Cost Defined over Digital Paths

In order to perform operations based on the distances we first need to define the notion of a topological distance.

Let \mathcal{G} be any nonempty set. We can measure distances between points in \mathcal{G} , which amounts to defining a real valued function on the Cartesian product $\mathcal{G} \times \mathcal{G}$ of \mathcal{G} with itself.

Let the function $\rho : \mathcal{G} \times \mathcal{G} \rightarrow R$ be called a distance if it is positive definite,

$$\rho(F_i, F_j) \geq 0, \text{ with } \rho(F_i, F_j) = 0 \text{ when } F_i = F_j, \quad (2)$$

and symmetric

$$\rho(F_i, F_j) = \rho(F_j, F_i), \text{ for all } F_i, F_j \in \mathcal{G}. \quad (3)$$

A distance is called a metric if additionally it satisfies the triangle inequality [5]

$$\rho(F_i, F_k) \leq \rho(F_i, F_j) + \rho(F_j, F_k), \text{ for all } F_i, F_j, F_k \in \mathcal{G}. \quad (4)$$

In digital image processing three basic distance functions are usually applied.

If $F_i = (F_i^1, F_i^2)$ and $F_j = (F_j^1, F_j^2)$ denote two image points ($F_i, F_j \in Z^2$) then we define the

- city-block distance

$$\rho_4(F_i, F_j) = |F_i^1 - F_j^1| + |F_i^2 - F_j^2|, \quad (5)$$

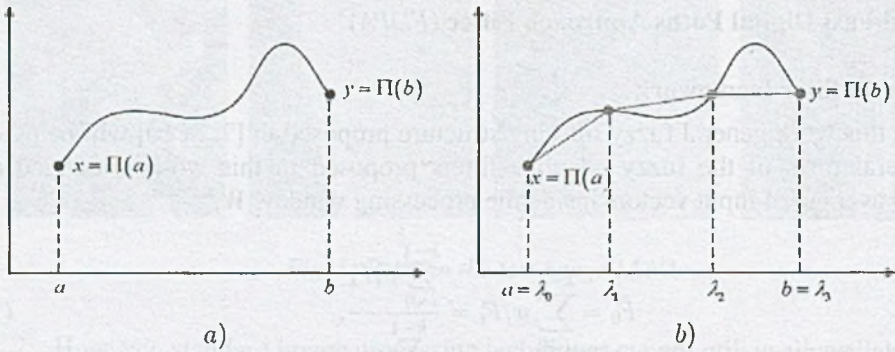


Fig. 2. a) Continuous path Π leading from the F_i to F_j , and b) increasing polygonal line on the path Π

- chessboard distance

$$\rho_8(F_i, F_j) = \max \{ |F_i^1 - F_j^1|, |F_i^2 - F_j^2| \}, \quad (6)$$

- Euclidean distance

$$\rho_E(F_i, F_j) = [(F_i^1 - F_j^1)^2 + (F_i^2 - F_j^2)^2]^{\frac{1}{2}}, \quad (7)$$

Using the city-block and chessboard distances we are able to define the two basic types of neighborhoods, 4-neighborhood \mathcal{N}_4 and 8-neighborhood \mathcal{N}_8

$$\mathcal{N}_4(F_i) = \{F_j, \rho_4(F_i, F_j) = 1\}, \quad \mathcal{N}_8(F_i) = \{F_j, \rho_8(F_i, F_j) = 1\}. \quad (8)$$

Let $\omega \in \{4, 8\}$. Two points $F_i, F_j \in Z^2$ are said to be in ω -neighborhood relation or to be \mathcal{N}_ω -adjacent if $F_i \in \mathcal{N}_\omega(F_j)$ or equivalently $F_j \in \mathcal{N}_\omega(F_i)$. This \mathcal{N}_ω -adjacency relation defines a graph structure on the image domain, called ω -adjacency graph. On the graph, a finite \mathcal{N}_ω -path can be defined as a sequence of points (p_0, p_1, \dots, p_n) such that for $i \in \{1, 2, \dots, n\}$ the point p_{i-1} is \mathcal{N}_ω adjacent to p_i . A path is called simple if $i \neq j$ implies that $p_i \neq p_j$. This is a very important property of a path, as it means that a path does not intersect itself [6].

Let us now introduce the concept of a geodesic distance.

Let us assume, that \mathbb{R}^2 is the Euclidean space, S is a subset of \mathbb{R}^2 and x, y are points belonging to set S . A path from x to y is a continuous mapping $\Pi: [a, b] \rightarrow S$, such that $\Pi(a) = x$ and $\Pi(b) = y$ (Fig. 2a). The point x is considered as starting point while y is the ending point on the path Π [3].

An increasing polygonal line P on the path Π is any polygonal line such that $P = \{\Pi(\lambda_i)\}_{i=0}^n, a = \lambda_0 < \dots < \lambda_n = b$. The length of the polygonal line P is considered to be the total sum of its constitutive line segments $L(P) = \sum_{i=1}^n \rho(\Pi(\lambda_{i-1}), \Pi(\lambda_i))$ where $\rho(x, y)$ is the distance between the points x and y , when a specific metric is adopted. A path Π from x to y is called rectifiable, if and only if $L(P)$, where P is an increasing polygonal line, is bounded. Its upper bound is called the length of the path Π (Fig. 2b).

The geodesic distance $\rho^S(x, y)$ between points x and y is the lower bound of the length of all paths leading from x to y which are totally included in S . If such paths do not exist, then the value of the geodesic distance is set to ∞ . In general $\rho^S(x, y) \geq \rho(x, y)$.

However, if the set S is convex, meaning that there are no points on the line between x and y that are not members of S , the geodesic distance satisfies $\rho^S(x, y) = \rho(x, y)$.

The notion of the path can be applied to a lattice, which is a set of discrete points in the plane, in our case the spatial locations of the image pixels. Let a digital lattice $\mathcal{H} = (F, \mathcal{N})$ be defined by F , which is the set of all points of the plane (pixels of a color image) and a neighborhood relation \mathcal{N} between the lattice points [13]. In the case of the ranked-type non-linear filters the processing window W forms a lattice where \mathcal{N} is defined through the window size.

A digital path $P = \{p_i\}_{i=0}^n$ defined on the lattice \mathcal{H} is a sequence of neighboring points $(p_{i-1}, p_i) \in \mathcal{N}$. The length $L(P)$ of the digital path $P \{p_i\}_{i=0}^n$ is simply $\sum_{i=1}^n \rho^{\mathcal{H}}(p_{i-1}, p_i)$, where $\rho^{\mathcal{H}}$ denotes the distance between two neighboring points of the lattice \mathcal{H} .

Constraining the paths to be totally included in a predefined set $W \in F$ yields the digital geodesic distance ρ^W .

An \mathcal{N}_ω -neighborhood system ($\omega = 4$ or $\omega = 8$) is considered in this work with a topological distance of 1 assigned between two neighboring points (Fig. 3).

Let us adopt the following notation, which will help us define the distance functions defined over digital paths.

The starting point of a path will be denoted as $p_0 = (x_0, y_0)$. Its neighbors will be denoted as $p_1 = (x_{u_1}, y_{v_1})$, which means that the neighbors are the second points of all digital paths originating at p_0 . Then the third point of a digital path starting at p_0 will be $p_2 = (x_{u_2}, y_{v_2})$ and so on, till the path reaches in n steps the ending point $p_n = (x_{u_n}, y_{v_n})$.

The set of all possible digital paths contained in W joining two points $x, y \in W$ will be denoted as $\Phi^W(x, y)$.

Two pixels x and y will be called connected (hereafter denoted as $x \leftrightarrow y$), if there exists a digital path $P^W(x, y)$ contained in the set W starting from x and ending at y .

If two pixels p_0 and p_n are connected by a geodesic path $P^{W,n} \{p_0, p_1, \dots, p_n\}$ of length n then let $\Lambda^{W,n} \{p_0, p_1, \dots, p_n\}$ be a function which measures the connection cost defined over the digital path linking the starting point p_0 and ending point p_n .

$$\Lambda^{W,n} \{p_0, p_1, p_2, \dots, p_n\} = f \{F(p_0), F(p_1), F(p_2), \dots, F(p_n)\} = f \{F(x_0, y_0), F(x_{u_1}, y_{v_1}), F(x_{u_2}, y_{v_2}), \dots, F(x_{u_n}, y_{v_n})\} \quad (9)$$

where f is a nonnegative scalar function of n vector variables.

The connection cost over the digital path $\Lambda^{W,n}$ will be defined as a measure of dissimilarity between color image pixels p_0, p_1, \dots, p_n forming a specific path linking p_0 and p_n [4, 18].

If a path joining two distinct points x, y , such that $F(x) = F(y)$ consists of lattice points of the same values, then the connection cost should be zero, otherwise $\Lambda^{W,n} > 0$.

Let us define a generalized connection cost function, based on the Distance Transform on the Curved Space [12, 18] introduced by Toivanen for the gray scale images.

For two given points $p_i = (x_{u_i}, y_{v_i})$ and $p_{i-1} = (x_{u_{i-1}}, y_{v_{i-1}})$, $i = 1, 2, \dots, n$, which are in neighborhood relation, let the generalized distance between the two points will be called connection cost

$$\Lambda^{W,1} \{p_{i-1}, p_i\} = \|F(p_i) - F(p_{i-1})\| + \rho^W(p_i, p_{i-1}) \quad (10)$$

The connection of a whole digital path p_0, p_1, \dots, p_n will be

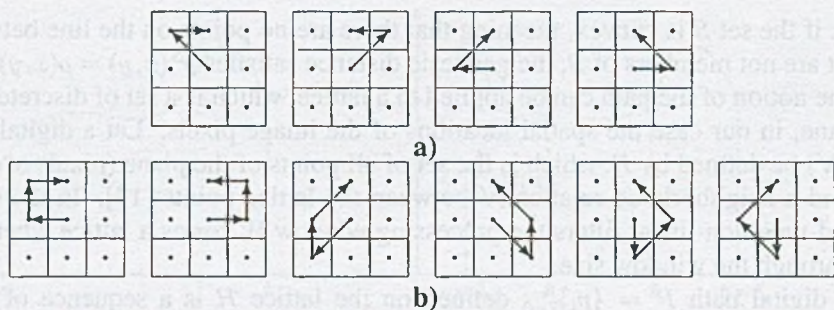


Fig. 3. Geodesic paths of length: a) length of 2; b) length of 3, connecting two neighboring points within a predefined window W of size 3×3 , when the 8-neighborhood system is applied

$$\Lambda^{W,n} \{p_0, p_1, \dots, p_n\} = \sum_{i=1}^n \left[\|F(p_i) - F(p_{i-1})\| + \rho^W(p_i, p_{i-1}) \right] \quad (11)$$

Similarly to the gray-scale case, we will call the minimal connection cost $\Gamma^{W,n}(x, y)$ of a path of length n linking two points $x, y \in W$, the n -geodesic between x and y :

$$\Gamma^{W,n}(x, y) = \min \left\{ \Lambda(\gamma), \gamma \in \Phi^{W,n} \right\} \quad (12)$$

In this way the n -geodesic is defined as the path of length n , which gives the minimal connection cost between two points linked by a digital path. If we take the minimum of the connection cost generated by all possible paths joining two points x and $y \in W$, then we get the generalized multichannel geodesic distance between these points

$$\Gamma^W(x, y) = \min_{n \in N} \left\{ \Gamma^{W,n}(x, y) \right\} = \min \left\{ \Lambda(p), p \in P^{W,n}(x, y), n \in N \right\}. \quad (13)$$

$\Gamma^W(x, y)$ defines the multidimensional distance transform, which is a generalization of the Distance Transform on Curved Space introduced by Toivanen for the gray-scale images.

In general, two distinct pixel's locations on the image lattice could be connected by many paths. Moreover the number of possible geodesic paths of certain length n connecting two distinct points depends on their locations, length of the path and the neighborhood system used (Figs. 3 and 4).

2.3. Similarity function

Let us now define a similarity function, analogous to a membership function used in fuzzy systems, between the starting point $x = p_0$ and point $y = p_1$ crossed by the digital path connecting pixel p_0 , its neighbor p_1 with all possible points p_n which can be reached in n steps from p_0 .

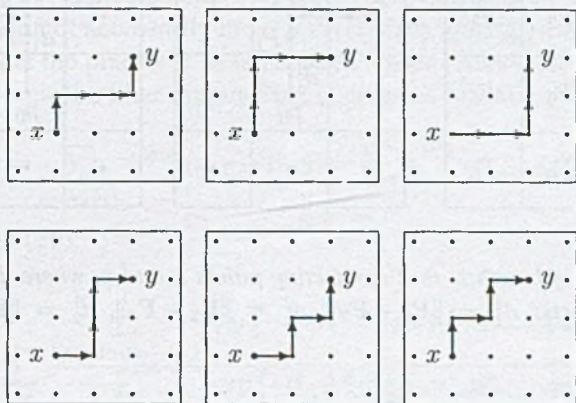


Fig. 4. There are six paths of length 4 connecting point x and y when the 4-neighborhood system is used (W of size 3×3)

The aim of taking into account the points p_2, \dots, p_n when calculating the similarity between p_0 and p_1 is to explore not only the direct neighborhood of p_0 but also to use the information on the local image structure.

This can be done by acquiring the information on the local image features investigating the connection costs of digital paths originating at p_0 , passing p_1 and then visiting successive points, till the path reaches length n . In this case the similarity function takes the form:

$$\mu^{W,n}(x, y) = \mu^{W,n}(p_0, p_1) = \sum_{P\{p_0, p_1, p_2^*, \dots, p_n^*\}} g\left(\Lambda^{W,n}\{p_0, p_1, p_2^*, \dots, p_n^*\}\right) \quad (14)$$

where $P\{p_0, p_1, p_2^*, \dots, p_n^*\}$ denotes the set of all paths originating at $x = p_0$ crossing $y = p_1$ and ending in p_n which are totally included in W , $\Lambda^{W,n}\{\cdot\}$ is a dissimilarity value along a specific path and $g(\cdot)$ is a smooth function of $\Lambda^{W,n}$.

The smooth function $g : (0; \infty] \rightarrow \mathbb{R}$ should satisfy following conditions:

1. g is a decreasing in $(0; \infty]$,
2. g is convex in $(0; \infty]$,
3. $g(0) = 1$,
4. $g(\Lambda) = 0$, when $\Lambda \rightarrow \infty$.

Several functions satisfying the above conditions have been proposed in the literature [9, 11, 14, 15]:

$$g_1(x) = e^{-\beta_1 x}, \quad \beta_1 \in (0; \infty), \quad (15)$$

$$g_2(x) = \frac{1}{1 + \beta_2 x}, \quad \beta_2 \in (0; \infty), \quad (16)$$

$$g_3(x) = \frac{1}{(1 + x)^{\beta_3}}, \quad \beta_3 \in (0; \infty), \quad (17)$$

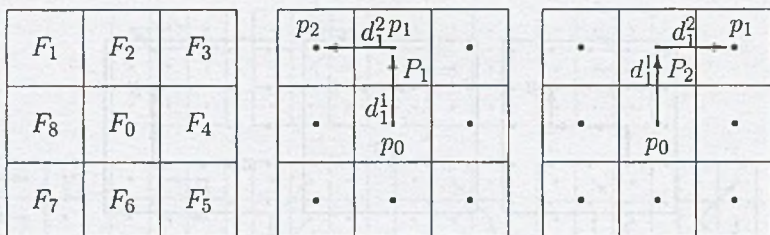


Fig. 5. Digital paths of length $n = 2$ connecting points x and y , where d_1^1 , d_1^2 , d_2^1 and d_2^2 are connection costs: $d_1^1 = \|F_0 - F_2\|$, $d_1^2 = \|F_2 - F_3\|$, $d_2^1 = \|F_0 - F_4\|$ and $d_2^2 = \|F_4 - F_3\|$

$$g_4(x) = 1 - \frac{2}{\pi} \arctan(\beta_4 x), \quad \beta_4 \in (0; \infty), \quad (18)$$

$$g_5(x) = \frac{2}{1 + e^{\beta_5 x}}, \quad \beta_5 \in (0; \infty), \quad (19)$$

$$g_6(x) = \frac{1}{1 + x^{\beta_6}}, \quad \beta_6 \in (0; 1), \quad (20)$$

$$g_7(x) = \begin{cases} 1 - \beta_7 x & \text{if } x < 1/\beta_7, \\ 0 & \text{if } x \geq 1/\beta_7, \end{cases} \quad \beta_7 \in (0; \infty). \quad (21)$$

In this work the exponential function of (15) is assumed so our similarity function takes the form:

$$\mu^{W,n}(x, y) = \mu^{W,n}(p_0, p_1) = \sum_{P\{p_0, p_1, p_2^*, \dots, p_n^*\}} \exp \left[-\beta \cdot \Lambda^{W,n} \{p_0, p_1, p_2^*, \dots, p_n^*\} \right] \quad (22)$$

where β is the filter design parameter.

For $n = 1$ and a square (3×3) window W the similarity function μ is defined as

$$\mu^{W,1}(x, y) = \exp \{ -\beta \|F(x) - F(y)\| \}, \quad (23)$$

and then if $F(x) = F(y)$, $\Lambda^{W,n}(x, y) = 0$, $\mu(x, y) = 1$, and for $\|F(x) - F(y)\| \rightarrow \infty$ then $\mu \rightarrow 0$ [8].

Figure 5 illustrates the calculation of the similarity function between two points connected by two paths of length $n = 2$. In this case

$$\Lambda_1^{W,2}(x, y) = d_1^1 + d_2^1, \quad \Lambda_2^{W,2}(x, y) = d_1^2 + d_2^2, \quad (24)$$

with d_1^1 , d_2^1 distances between neighboring points on the path P_1 defined according to (11), while d_1^2 , d_2^2 are similarly defined on P_2 . The total similarity value can be expressed as follows:

$$\mu^{W,2} = \left[\exp \left(-\beta \cdot \Lambda_1^{W,2} \right) + \exp \left(-\beta \cdot \Lambda_2^{W,2} \right) \right] \quad (25)$$

A normalized form of the similarity function can be defined as follows:

$$\psi^{W,n}(x, y) = \psi^{W,n}(p_0, p_1) = \frac{\sum_{P\{p_2, p_3, \dots, p_n\}} \exp \left[-\beta \cdot \Lambda^{W,n} \{p_0, p_1, p_2, \dots, p_n\} \right]}{\sum_{P\{p_0, p_1^*, p_2^*, \dots, p_n^*\}} \exp \left[-\beta \cdot \Lambda^{W,n} \{p_0, p_1^*, p_2^*, \dots, p_n^*\} \right]} \quad (26)$$

where $P\{p_0, p_1, \dots, p_n\}$ denotes paths joining $x = p_0$ and p_n crossing $y = p_1$, whereas $\{p_0, p_1^*, p_2^*, \dots, p_n^*\}$ do not necessarily cross $y = p_1$ when joining p_0 and p_n .

Assuming that the pixel $x = p_0$ is the pixel under consideration, with $F(y)$ representing the pixel $y = p_1$ the filter output $\hat{F}(x)$ is given as follows:

$$\hat{F}(x) = \sum_{y \sim \mathcal{N}_8(x)} \psi^{W,n}(x, y) \cdot F(y) = \sum_{p_1} \psi^{W,n}(p_0, p_1) \cdot F(p_1), \quad (27)$$

and combining with (26):

$$\hat{F}(p_0) = \sum_{p_1} \frac{\sum_{P\{p_0, p_1, p_2, \dots, p_n\}} \exp[-\beta \cdot \Lambda^{W,n}\{p_0, p_1, p_2, \dots, p_n\}]}{\sum_{P\{p_0, p_1^*, p_2^*, \dots, p_n^*\}} \exp[-\beta \cdot \Lambda^{W,n}\{p_0, p_1^*, p_2^*, \dots, p_n^*\}]} \cdot F(p_1) \quad (28)$$

3. Spatio-Temporal Fast Digital Paths Approach Filter (FDPA-3D)

Our Spatio-temporal approach extends idea of digital paths in the image lattice into three dimensional space. Paths in time can be interpreted as object trajectories through subsequent frames.

In general spatio-temporal algorithm extension introduces only one difference shape of the processing window W . Figure 6 shows 3D masks used for video processing using 4 and 8-neighborhood. In this work simple mask of $3 \times 3 \times 3$ with 8-neighborhood will be used.

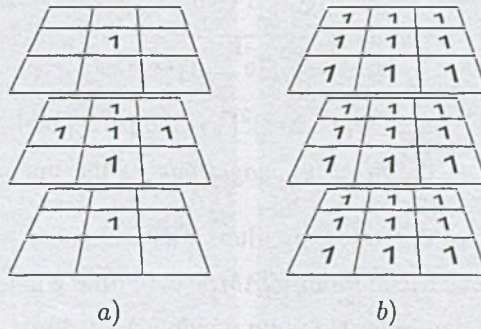


Fig. 6. Examples of spatio-temporal masks W for a) 4-neighborhood and b) 8-neighborhood systems

4. Simulation Results

Our new filter efficiency was tested on numerous video sequences. Subjective results were obtained from original noisy video sequences, however some synthetic tests with artificial noise were also performed.

Objective quality measures such as the *Root Mean Squared Error* (RMSE), the *Signal to Noise Ratio* (SNR), the *Peak Signal to Noise Ratio* (PSNR), the *Normalized Mean Square Error* (NMSE) and the *Normalized Color Difference* (NCD) [11] were

used for the analysis. All those objective quality measures were calculated for the sequence of the filtered images. The following formulas define each measure for each video frame separately:

$$RMSE = \sqrt{\frac{1}{NML} \sum_{i=0}^{N-1} \sum_{j=0}^{M-1} \sum_{l=1}^L (F^l(i, j) - \hat{F}^l(i, j))^2} \quad (29)$$

$$NMSE = \frac{\sum_{i=0}^{N-1} \sum_{j=0}^{M-1} \sum_{l=1}^L (F^l(i, j) - \hat{F}^l(i, j))^2}{\sum_{i=0}^{N-1} \sum_{j=0}^{M-1} \sum_{l=1}^L F^l(i, j)^2} \quad (30)$$

$$SNR = 10 \log \left[\frac{\sum_{i=0}^{N-1} \sum_{j=0}^{M-1} \sum_{l=1}^L F^l(i, j)^2}{\sum_{i=0}^{N-1} \sum_{j=0}^{M-1} \sum_{l=1}^L (F^l(i, j) - \hat{F}^l(i, j))^2} \right] \quad (31)$$

$$PSNR = 20 \log \left(\frac{255}{RMSE} \right), \quad (32)$$

where M , N are the image dimensions, and $F^l(i, j)$ and $\hat{F}^l(i, j)$ denote the l^{th} component of the original image vector and its estimation at pixel (i, j) , respectively.

The NCD perceptual measure is evaluated over the uniform $L^*u^*v^*$ color space. The difference measure is given as follows:

$$NCD = \frac{\sum_{i=0}^{N-1} \sum_{j=0}^{M-1} \Delta E_{Luv}}{\sum_{i=0}^{N-1} \sum_{j=0}^{M-1} E_{Luv}^*}, \quad (33)$$

where $\Delta E_{Luv} = [(\Delta L^*)^2 + (\Delta u^*)^2 + (\Delta v^*)^2]^{\frac{1}{2}}$ is the perceptual color error and $E_{Luv}^* = [(L^*)^2 + (u^*)^2 + (v^*)^2]^{\frac{1}{2}}$ is the norm or magnitude of the uncorrupted original image pixel vector in the $L^*u^*v^*$ space.

The performance of the following filters was evaluated:

- Temporal Arithmetic Mean Filter - TAMF (with time window of size 3),
- Spatial Vector Median Filter [1] (with window 3×3 and L_1 norm),
- Spatial Fast Digital Paths Approach FDPA (with paths of size 2 and $\beta = 15$),
- Spatio-temporal Vector Median Filter - VMF3D (with window $3 \times 3 \times 3$ and L_1 norm),
- Spatio-temporal Fast Digital Paths Approach FDP3D (with paths of size 2 and $\beta = 15$)

Figure 7 and 8 show filtering results of single frame from noisy video sequences *The Car* and *The Jongleur*. Both sequences contain the small moving objects and relatively big static areas. Temporal filters are capable of perfect smoothing of static areas, however they produce ghosting artifacts. On the other hand spatial filters are 'too weak' to remove all artifacts. The proposed algorithm smooths static areas, preserves edges and reduces ghosting artifacts to negligible level (unnoticeable in moving sequence).

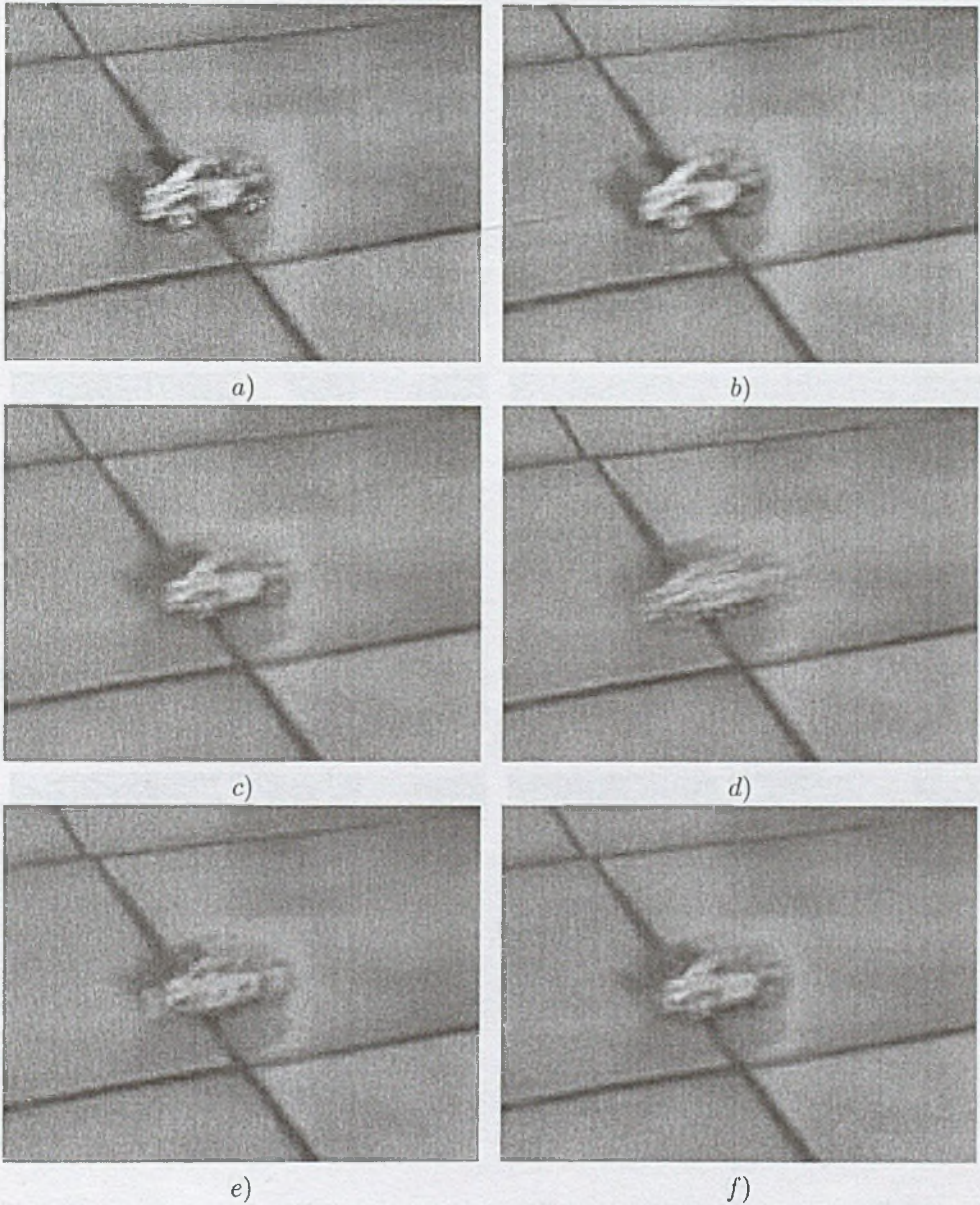


Fig. 7. Comparison of the efficiency of the tested filters applied to the noisy sequence *The Car* (Frame no. 96): a) crop from the original noisy frame, b) spatial VMF, c) spatial FDPA filter, d) Temporal mean filter (TAMF), e) spatio-temporal vector median (VMF3D) and f) spatio-temporal FDPA (FDPA3D)

Figure 9 presents comparison of the efficiency of the tested filters applied to the sequence *Rabbit* corrupted with mixed Gaussian ($\sigma = 15$) and impulsive noise (5%) while objective quality measures are collected in Tab. 1. It is clear that presented technique outperforms compared filters especially when applied to videos corrupted with heavy and mixed noise.

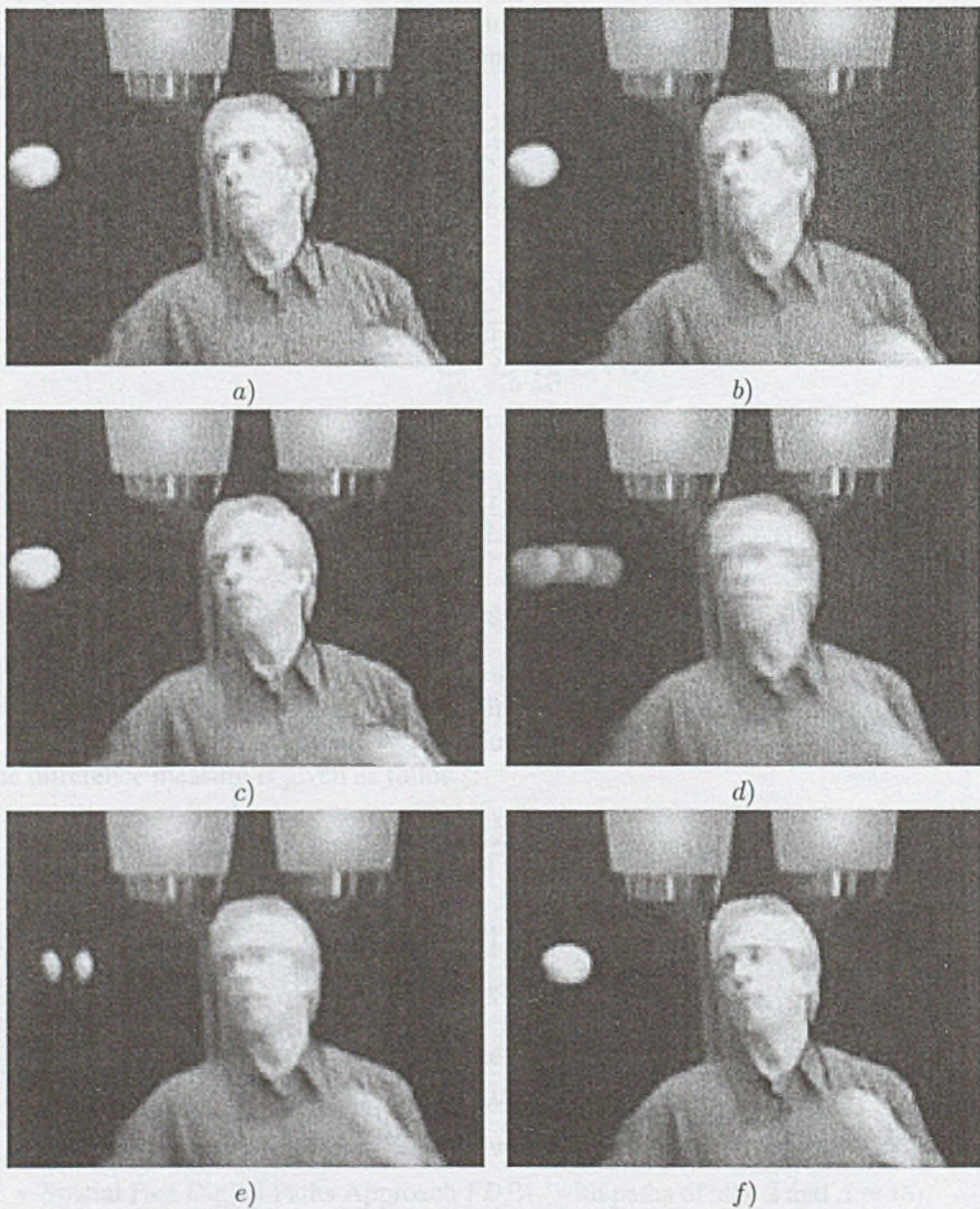


Fig. 8. Comparison of the efficiency of the tested filters applied to the noisy sequence Jongluer (Frame no. 52): a) crop from the original noisy frame, b) spatial VMF, c) spatial FDPA filter, d) Temporal mean filter (TAMF), e) spatio-temporal vector median (VMF3D) and f) spatio-temporal FDPA (FDPA3D)

After closer inspection it can be noticed that Spatio-Temporal FDPA filter also eliminates some compression artifacts (Fig. 10).

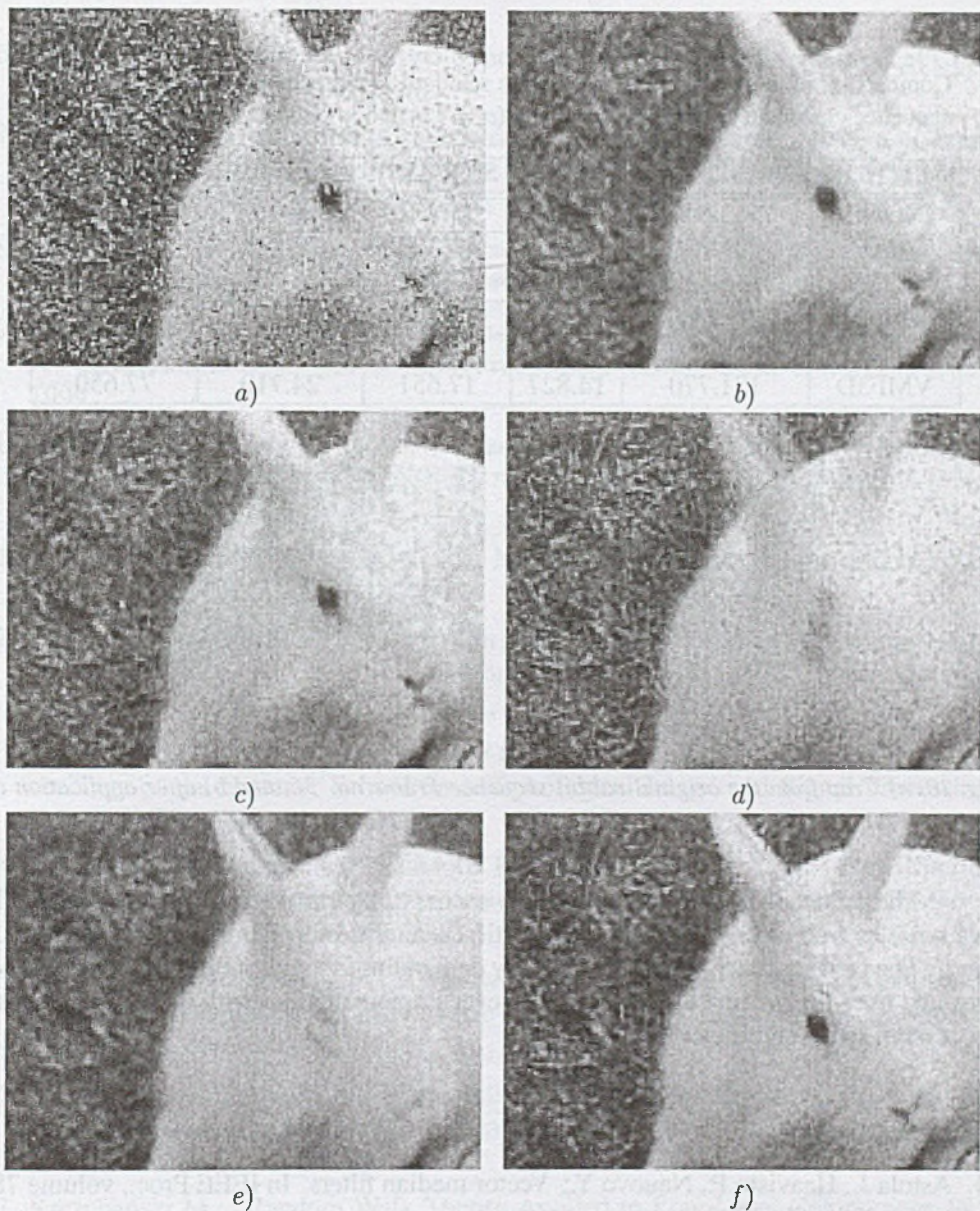


Fig. 9. Comparison of the efficiency of the tested filters applied to the sequence Rabbit corrupted with mixed Gaussian ($\sigma = 15$) and impulsive noise (5%) - Frame no. 36: a) crop from the corrupted frame, b) spatial VMF, c) spatial FDPA filter, d) Temporal mean filter (TAMF), e) spatio-temporal vector median (VMF3D) and f) spatio-temporal FDPA (FDPA3D)

5. Conclusions

This paper has introduced a new efficient filter for color video denoising. Presented technique utilizes fuzzy membership functions over vectorial inputs connected via digital paths in spatio-temporal domain.

Table 1

Comparison of the new algorithm with the standard some techniques using the rabbit sequence corrupted with mixed Gaussian ($\sigma = 15$) and impulsive noise (5%) (Fig. 9)

METHOD	NMSE [10^{-3}]	RMSE	SNR [dB]	PSNR [dB]	NCD [10^{-4}]
NONE	581.840	27.288	12.352	19.411	120.540
TAMFT	284.700	19.089	15.456	22.515	109.580
FDPA	114.510	12.106	19.411	26.471	66.349
FDPA3D	90.704	10.774	20.424	27.483	62.235
VMF	158.450	14.241	18.001	25.060	74.535
VMF3D	171.770	14.827	17.651	24.710	77.650



Fig. 10. a) Crop from the original rabbit sequence Frame no. 36, and b) after application of FDPA3D

The proposed filtering technique can successfully eliminate Gaussian and impulsive noise as well as digital compression artifacts and its outperforms compared filters.

The new approach is computationally demanding, so without further optimization it can be used for off-line processing. However implementation with GPU can increase processing speed significantly.

BIBLIOGRAPHY

1. Astola J., Haavisto P., Neuovo Y.: Vector median filters. In IEEE Proc., volume 78, pages 678–689, 1990.
2. Bennett E. P., McMillan L.: Video enhancement using per-pixel virtual exposures. ACM Trans. Graph., 24(3):845–852, 2005.
3. Borgefors G.: Distance transformations in digital images. Computer Vision, Graphics, and Image Processing, 34:344–371, 1986.
4. Cuisenaire O.: Distance transformations: fast algorithms and applications to medical image processing. PhD thesis, Universite Catholique de Louvain, Oct. 1999.
5. Kiselman C. O.: Regularity properties of distance transformations in image analysis. Computer Vision and Image Understanding, 64(3):390–398, November 1996.

6. Malgouyres R.: Homotopy in two-dimensional digital images. *Theoretical Computer Science*, 230:221–233, 2000.
7. Plataniotis K. N., Androutsos D., Venetsanopoulos A. N.: Colour image processing using fuzzy vector directional filters. In *Proc. of the IEEE Workshop on Nonlinear Signal/Image Processing*, Greece, pages 535–538, 1995.
8. Plataniotis K. N., Androutsos D., Venetsanopoulos A. N.: Fuzzy adaptive filters for multichannel image processing. *Signal Processing Journal*, 55(1):93–106, 1996.
9. Plataniotis K. N., Androutsos D., Venetsanopoulos A. N.: Adaptive fuzzy systems for multichannel signal processing. *Proceedings of the IEEE*, 87(9):1601–1622, 1999.
10. Plataniotis K. N., Androutsos D., Vinayagamoorthy S., Venetsanopoulos A. N.: Color image processing using adaptive multichannel filters. *IEEE Trans. on Image Processing*, 6(7):933–950, 1997.
11. Plataniotis K. N., Venetsanopoulos A. N.: *Color Image Processing and Applications*. Springer Verlag, August 2000.
12. Preteux F., Merlet N.: New concepts in mathematical morphology: the topographical distance function. In P. D. Gader and E. R. Dougherty, editors, *Proceedings of SPIE*, volume 1568, pages 66–77, 1991.
13. Schmitt M.: Lecture notes on geodesy and morphological measurements. In *Proceedings of the Summer School on Morphological Image and Signal Processing*, Zakopane, Poland, pages 36–91, 1995.
14. Smolka B., Chydzinski A., Plataniotis K., Venetsanopoulos A. N.: New filtering technique for the impulsive noise reduction in color images. *Mathematical Problems in Engineering*, 2004(1):79–91, 2004.
15. Smolka B., Chydzinski A., Wojciechowski K., Plataniotis K., Venetsanopoulos A. N.: On the reduction of impulsive noise in multichannel image processing. *Optical Engineering*, 40(6):902–908, 2001.
16. Szczepanski M., Smolka B., Plataniotis K. N., Venetsanopoulos A. N.: On the geodesic paths approach to color image filtering. *Signal Processing*, 83(6):1309–1342, June 2003.
17. Szczepański M.: *Random Walk Theory Applied to Low Level Color Image Processing*. PhD thesis, department of Automatic, Electronics and Computer Science, Silesian University of Technology, Gliwice, Poland, 2003.
18. Toivanen P. J.: New geodesic distance transforms for gray scale images. *Pattern Recognition Letters*, 17:437–450, 1996.

Recenzent: Dr hab. inż. Wiesław Kotarski

Omówienie

W niniejszej pracy przedstawiono nową, efektywną metodę filtracji barwnych sekwencji wideo - czasowo-przestrzenny filtr FDPA (*FDPA3D*). Grupy pikseli obrazu formują ścieżki cyfrowe odzwierciedlające struktury przestrzenne występujące w obrazie, podczas gdy obiekty występujące w kolejnych klatkach tworzą trajektorie. Zaproponowany algorytm wykorzystuje ideę ścieżek cyfrowych w trójwymiarowej przestrzeni.

Ścieżki cyfrowe eksplorują struktury obrazu zarówno w czasie, jak i przestrzeni, co zapewnia doskonale zachowanie detali obrazu oraz zapobiega powstawaniu artefaktów związanych z uśrednianiem ruchomych obiektów pomiędzy kolejnymi klatkami.

Skuteczność prezentowanego algorytmu przetestowano zarówno z wykorzystaniem naturalnie zaszumionych sekwencji wideo, jak i materiału z zakłóceniem syntetycznym. W testowanych sekwencjach występowały sceny statyczne oraz szybko poruszające się obiekty.

otrzymane rezultaty pokazują, że zaprezentowana technika skutecznie usuwa szum Gaussowski, impulsowy, efekt ziarna oraz artefakty kompresji cyfrowej. Opracowany filtr *FDPA3D* doskonale zachowuje, a nawet poprawia krawędzie w poszczególnych klatkach, nie powodując równocześnie rozmycia ruchomych obiektów.